Effect of Thermal History on Mechanical Properties of Polyetheretherketone below the Glass Transition Temperature

PEGGY CEBE,* SHIRLEY Y. CHUNG, and SU-DON HONG†,
Applied Sciences and Microgravity Experiments Section, Jet Propulsion Laboratory, California Institute of Technology, Pasadena, California 91109

Synopsis

Tensile properties of polyetheretherketone (PEEK) have been studied at 125, 25, and −100°C for thin films prepared with different thermal histories. Initial morphology was controlled by rate of cooling from the melt. Amorphous films resulted from quenching the melt, while semicrystalline films were obtained by cooling the melt at different rates, or by crystallization of the rubbery amorphous state. The films were characterized using density, X-ray scattering, differential scanning calorimetry, and infrared spectroscopy. Scanning electron microscopy was used to examine fracture surfaces. Degree of crystallinity and rate of cooling from the melt affected the tensile properties at all test temperatures. For films with nearly the same degree of crystallinity, those which were more slowly cooled from the melt fractured at the lowest strain. The amorphous films were most tough, drawing to 233% at −100°C and to over 500% at 125°C. Films crystallized from the rubbery amorphous state had stress–strain behavior intermediate between that of the amorphous and melt-crystallized films at all test temperatures. Density measurements on the drawn material indicate that void formation occurs simultaneously with the formation of fibrillar crystals. Necking resulted in density increases for amorphous films, and density decreases for the semicrystalline films.

INTRODUCTION

Polyetheretherketone (PEEK) is an aromatic thermoplastic polymer with applications as the matrix material in high performance composites. The PEEK repeat unit is (ϕ-o-ϕ-o-ϕ-co) in planar zig-zag conformation.[1] Due to the relatively stiff backbone PEEK shows excellent high temperature stability. It has a glass transition temperature of 145°C, a melting point of 335°C, and continuous use temperature of 200°C.[2]

In addition to its high temperature properties, PEEK is resistant to chemical attack and to high energy radiation.[2,3] At room temperature, PEEK is completely soluble in very strong acids, such as trifluoro-methanesulfonic (triflic) acid or concentrated sulfuric acid. Recent work has shown that sulfonation of the phenyl groups occurs[4] which may limit the use of these solvents. Other solvents exist which can be used at elevated temperatures. Diaryl sulfones have been used to dissolve PEEK at its melting point,[2] and, recently, Lovinger and Davis[5] have produced PEEK single crystals from

* To whom communications should be addressed.
† Present address: 1625 Olympic Blvd., Suite 800, Los Angeles, CA 90015.

Journal of Applied Polymer Science, Vol. 33, 487–503 (1987)
 CCC 0021-8995/87/020487-17$04.00

1-chloronaphthalene and benzophenone at their boiling points. However, to produce bulk samples for mechanical testing, it is easiest to process PEEK from the melt, and both amorphous and semicrystalline films can be obtained by varying the thermal treatment of the melt.[6,7]

The degree of crystallinity and crystal perfection of PEEK films depends on the thermal history imparted during processing. An amorphous material results from rapid quenching of the melt.[6] A semicrystalline material is formed by isothermal crystallization, slow cooling of the melt, or by crystallization of the rubbery amorphous state.[6,7] Our previous research into the crystallization kinetics of PEEK indicated that degree of crystallinity depended greatly upon the crystallization conditions.[7] For example, when PEEK was crystallized from the rubbery amorphous state, the degree of crystallinity was much smaller than that obtained by melt crystallization, even when the crystallization rates were comparable. In addition, the rate at which PEEK was cooled from the melt, or heated from the rubbery state,[8] had a large effect upon the crystal perfection.

Recent work on characterization of PEEK neat resin has included structure,[1,2,9] morphology,[10] effect of solvents,[2,4] and effect of radiation on crystallinity.[3] Several studies of mechanical properties have been concerned with PEEK composite materials.[11,12] However, mechanical properties of the neat resin are now beginning to receive attention, since it is essential to characterize the behavior of the resin to understand fully the composite properties. The work of Stober et al.,[13] considers dynamic mechanical relaxation behavior for wet and dry PEEK. Effect of physical aging on mechanical properties has been studied by Kemmish and Hay.[14] Jones et al.[15] consider a range of mechanical tests for the neat resin to provide guidelines for use of PEEK in engineering applications. Sasuga and Hagiwara[16] have reported on molecular relaxation before and after irradiation. Recent work in our laboratory[17] considers the room temperature properties of the neat resin.

In the present paper, we extend our previous research and report the results of tensile testing of PEEK neat resin films at three temperatures below the glass transition temperature. Thermal history imparted during processing has a large effect on the mechanical properties even at temperatures far below T_g. For melt crystallized films having about the same degree of crystallinity, the rate of cooling had a drastic effect on tensile properties at all test temperatures.

EXPERIMENTAL

Sample Preparation

Thin films were pressed from free flowing granules of PEEK (supplied by ICI Americas, Inc.) that had been dried under vacuum at 110°C. The material used in this study had a relative viscosity of 2.4, measured at 25°C in 96% H_2SO_4 at a concentration of 1 g/100 mL. Pellets were molded between ferrotype plates at 370°C under 20,000 psi for several minutes. To form amorphous films, the molten samples were removed from the press and quenched into cold water. Only clear, smooth and stress-free areas were used in subsequent tests. The films were 0.005–0.010 cm thick before testing.

The amorphous film was cut into strips and heated in a Mettler FP80 hot stage to obtain films crystallized from the rubbery amorphous state. Thin strips were heated on glass slides to 140°C and allowed to equilibrate briefly, and then heated at 20°C/min to 180°C and crystallized at that temperature for 1 h.

Two different methods were used to crystallize films from the melt. In the first treatment, samples were cooled slowly from the melt by leaving them in the hot press overnight with the heating unit turned off. These samples cooled slowly to room temperature in about 16 h. For the second treatment, samples were withdrawn from the press in the molten state and cooled in air to room temperature in about 2–3 h. The four sample types will be referred to as Q (quenched amorphous), C180 (quenched then crystallized at 180°C), SC (slowly cooled from the melt), and AC (air cooled from the melt).

Sample Characterization

Density was measured in calcium nitrate solution. Crystallinities were calculated assuming 1.264 g/cc for the amorphous density and 1.378 g/cc for the crystal density.[1]

Thermal analysis was performed using a DuPont 1090 thermal analyzer operating at a heating rate of 20°C/min. For calculations of degree of crystallinity, 130 J/g heat of fusion was assumed[6] for the perfect crystal phase.

A Siemens D-500 diffractometer was used to record the wide angle X-ray scattering patterns in reflection mode using CuK_α radiation. A step scan interval of $2\theta = 0.1$ degree was used with a 7 s per interval scanning rate.

Fourier transform infrared spectroscopy was performed in transmission, using an Analect 6160 spectrometer. The area ratio of the 966 and 952 cm^{-1} peaks was used to determine the degree of crystallinity.

Mechanical testing was done on an Instron tensile tester equipped with an environmental chamber. Tests were performed at a constant crosshead speed of 0.2 in/min, at 125, 25, and −100°C. Strain was computed from crosshead movement for samples taken to failure, and from separation of fiducial marks for the unbroken test pieces. Stress was calculated based on the initial cross-sectional area of the undrawn film.

RESULTS AND DISCUSSION

Sample Characterization

In Figures 1(a) and (b) results of FTIR analysis are shown. The spectra of the four sample films taken in transmission are shown in Figure 1(a). Whereas Chalmers et al.[18] used the peak height ratio to determine the crystallinity, the area under the peak is usually a better indicator of absorber concentration. Area measurement tended to be more reproducible, especially at low degree of crystallinity where the 966 cm^{-1} peak had no clear maximum.

In Figure 1(b) the ratio of the areas under the 966 and 952 cm^{-1} peaks is shown as a function of the crystallinity. The dashed line is the calibration curve deduced from measurements on a separate set of films. The open circles represent the four films used in this study, placed on the dashed line according

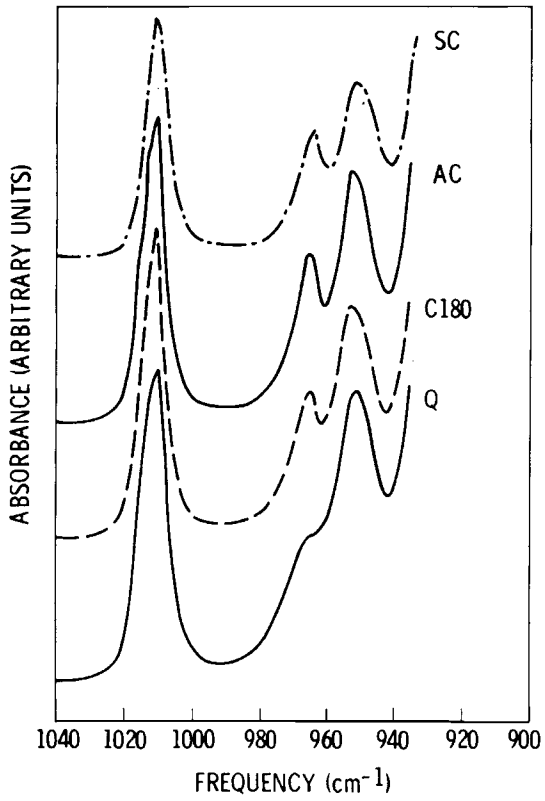

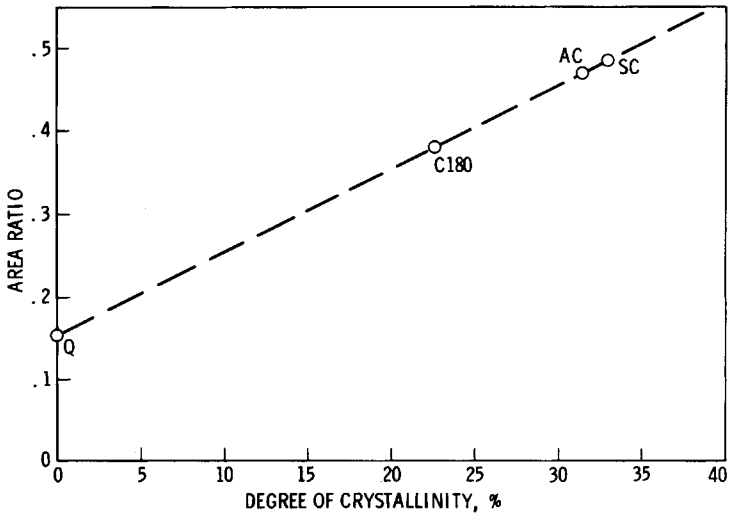

Fig. 1. (a) Infrared absorbance vs. frequency for PEEK films, transmission mode. (b)Ratio of 966 to 952 cm^{-1} peak area vs. crystallinity. Calibration curve (- - -) was determined from an independent set of films. Measured area ratios for Q, C180, AC, and SC are shown with open circles. See Table I for comparison of crystallinities as determined from other methods.

TABLE I
Degree of Crytallinity Determined by Density, WAXS, DSC, and FTIR

Sample	Volume fraction of crystallinity (%)			
	X_c (density)	X_c (WAXS)	X_c (DSC)	X_c (FTIR)
Q	0.9	—	1.4	0
C180	23.7	23.6	22.2	22.5
AC	32.9	29.6	27.4	31.5
SC	31.6	32.6	32.0	33.0

TABLE II
Peak Melting Temperatures and Lamellar Thickness for PEEK Films

Sample	T (lower °C)	T (upper °C)	l (Å)
C180	202	335.2	23
AC	270	335.5	48
SC	305	337.0	53

to their measured area ratios. Crystallinity can be deduced from the corresponding abscissa values. Crystallinity was also determined using density, WAXS, and DSC. A comparison of these results is shown in Table I. Very good agreement was obtained among the four methods.

In Table II the melting points (from Figure 2 endotherms) and lamellar thickness l are listed for the semicrystalline films. T_m (lower) corresponds to the low temperature secondary endotherm, while T_m (upper) corresponds to the main high temperature endotherm. Lamellar thickness was calculated from the X-ray long period L, using $l = LX_c$. For melt-crystallized films SC and AC, the lamellar thickness and high temperature melting point agree well with the data of Blundell and Osborn (see Fig. 5 of Ref. 6).

All three semicrystalline films exhibited both high and low temperature endotherms. For C180, this secondary melting peak occurred at 202°C, 20°C above the crystallization temperature. For the melt-crystallized films, the secondary endotherm was closer to the main melting point. The endothermic response of the semicrystalline films is shown in Figure 3. In all cases, the area under the low temperature endotherm is very small compared to the main endotherm and represents melting of about 10–14% of the crystals. Thus, in each semicrystalline film, there exists at room temperature a population of small imperfect crystals which melt just above their formation temperature.

Some reorganization occurs during the DSC scan of film C180. The melting of the least perfect crystals at 202°C is followed by a shift in the baseline, indicating an exothermic response. Reorganization during the scan can be expected for C180, since, as a result of the low initial crystallization temperature, additional crystallization may occur as the temperature is increased. No similar behavior is observed in the melt-crystallized films. Their processing condition allows crystals to form over a wide range of temperatures during cooling, and when these films are subsequently heated, only an endothermic response can be seen. For both AC and SC, melting begins at about 240°C.

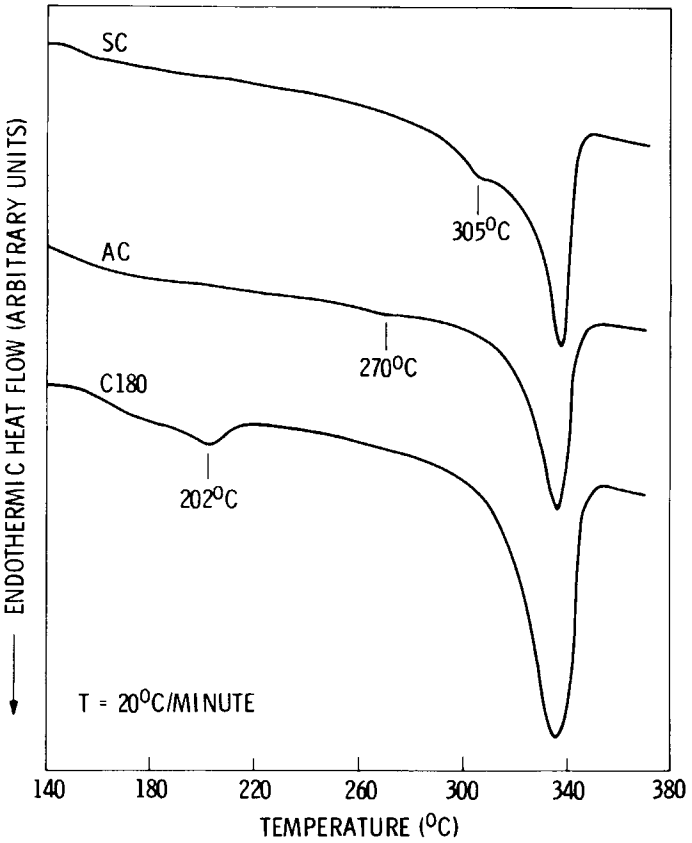

Fig. 2. DSC scans at 20°C/min of PEEK films C180, AC, and SC.

The secondary endotherm in SC is closer to the main endotherm, indicating that the average lamellar thickness is greater in SC, a result also borne out by small angle X-ray results.

Wide angle X-ray scattering curves are shown in Figure 3(a) for the quenched and cold crystallized films, and in Figure 3(b) for the melt-crystallized films. The crystal reflections from C180 are very broad and poorly resolved, indicative of an imperfect crystal structure. The crystal reflections from SC and AC are similar, though the peaks from AC are broader (larger full width at half maximum) than those of SC. All three films had a shoulder at $2\theta = 14°$ which was not present in any amorphous film tested. This broad scattering at low angles is attributed to stresses in the amorphous material imparted during the crystallization process. Though AC and SC contain about the same volume fraction of crystallinity, the crystals of AC are smaller, as evidenced by the lower melting points, slightly broader WAXS pattern, and thinner lamellae.

To summarize, the processing history imparted different bulk crystallinities, as well as different microstructures in the four films studied. The melt-crystallized films had nearly the same degree of crystallinity but differed in their endothermic response, wide angle scattering, and lamellar thickness. The slowly cooled film appears to have a greater degree of crystal perfection, due

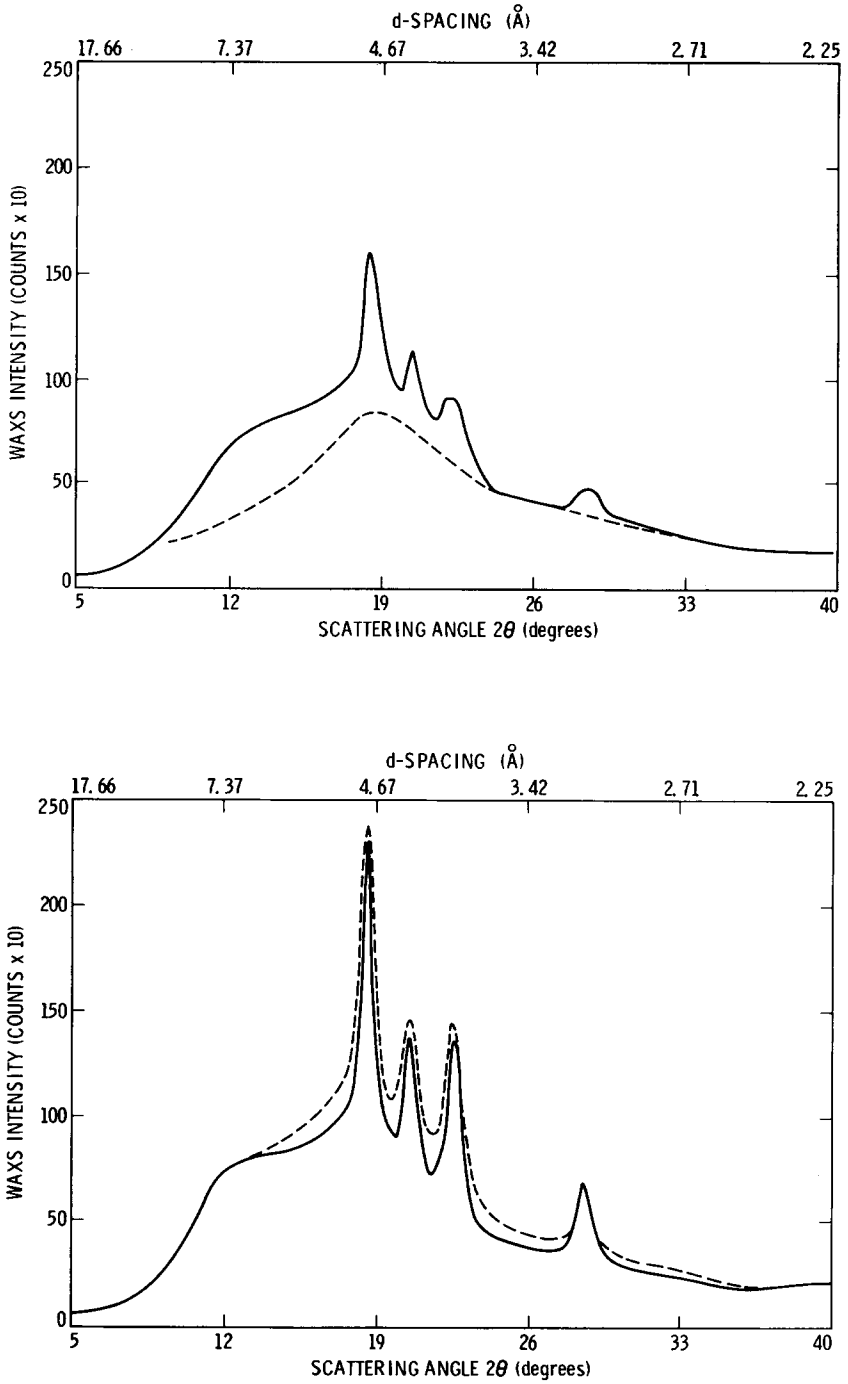

Fig. 3. WAXS intensity vs. scattering angle for: (a) Q (- - -) and C180 (——), upper figure; (b) AC (- - -) and SC (——).

both to the slightly thicker lamellae and to a probable reduction in defect concentration within the lamellae. Film C180 had lower crystallinity and more imperfect crystal microstructure. In the next section, we consider the effects of processing-induced microstructure on the tensile properties.

Mechanical Testing

Stress–Strain at 125°C

Stress–strain behavior at 125°C is shown in Figure 4. The effect of crystallinity is seen in the increased stresses for yield and for neck propagation in the semicrystalline films, compared with the Q film. The breaking strain, while always subject to the existence of defects in the samples, decreases as the degree of crystallinity increases.

Film Q has a well-defined yield point followed by a steep drop in stress before necking begins. The neck forms at constant stress level and runs completely to the grips. Strain hardening begins at about 100% strain. Film Q was extended to over 500%, at which point the machine extension limit was reached. Mechanical properties of the four films are summarized in Table III for all test temperatures.

At the other extreme, film SC yielded at this temperature and formed a short neck. This film was the least tough at 125°C but could still be drawn to 74% before failure. The other semicrystalline films exhibited very tough behavior when compared to the Q film, especially in the low strain regime. Film AC had no distinct yield point, but did form a neck and extended at

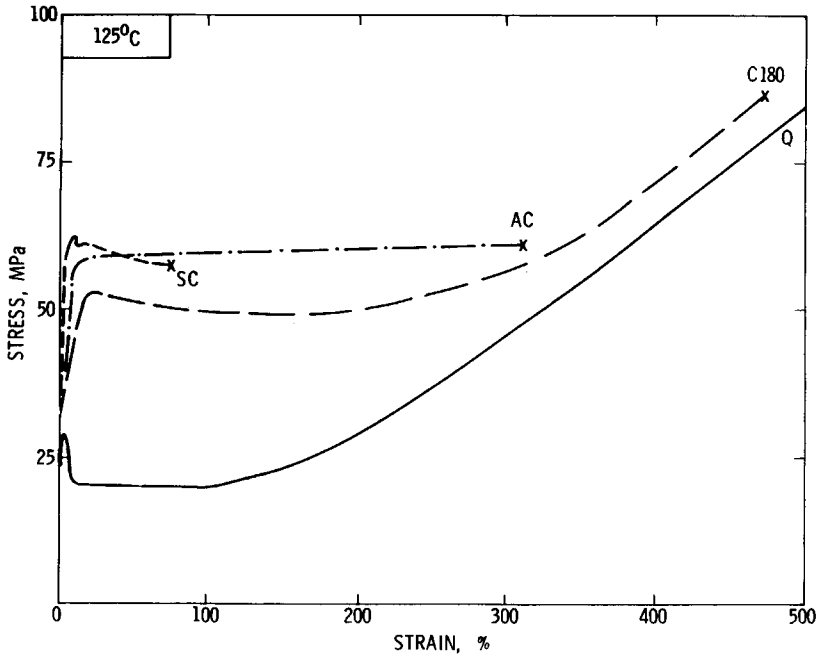

Fig. 4. Engineering stress–strain response of PEEK films drawn at 125°C.

TABLE III
Mechanical Properties of PEEK Films having Different Thermal Histories

Sample	Test temp (°C)	Yield stress (MPa)	Yield strain (%)	Breaking stress (MPa)	Breaking strain (%)	Young's modulus (GPa) (at 1% ϵ)
Q	125	31	3.0	> 85[a]	> 496[a]	1.4
	25	66	7.6	115	271	1.8
	−100	132	7.7	142	233	3.0
C180	125	52	6.0	87	472	1.3
	25	83	8.5	95	243	1.5
	−100	163	11.3	140	70	3.6
SC	125	61	7.8	57	74	1.9
	25	95	7.0	85	28	1.8
	−100	[b]	[b]	203	77	2.2
AC	125	55	5.5	66	305	1.4
	25	106	9.0	97	165	2.0
	−100	189	7.0	153	39	4.5

[a] Reached maximum extension of the machine.
[b] Brittle fracture, no yield.

constant stress. AC broke before any strain hardening occurred. Since AC and SC have very nearly the same degree of crystallinity, the differences in tensile properties must be associated with the degree of perfection resulting from the different cooling rates. Way et al.[19] have suggested that an increase in spherulite size, which would result from a slow cooling treatment, would cause embrittlement and low strain-to-break.

The C180 film has behavior intermediate between that of AC and Q. C180 has a shallow yield point, and in the low strain region (up to about 200%) behaves like AC. In the high strain region, above 300%, C180 strain hardens like the Q film. If the slope of the strain hardening region is used as a rough indication of the material modulus after drawing, then C180 and Q film have similar properties after high temperature drawing.

For drawing at a temperature near T_g, we see that an increased degree in crystallinity results in increased yield stress and stress for neck formation. The slowly cooled film breaks at comparatively low strain, while the air cooled film draws to a much greater extension. AC does not strain harden, an indication that the crystals formed during melt crystallization act as (thermoreversible) crosslinks. In the neck forming region, amorphous material becomes extended. However, in AC, after necking, the amorphous chains are unable to become oriented any further. Film C180, on the other hand, does harden after necking. This we attribute to the poorly developed crystals which are not effective in serving as crosslinking sites. During the hardening process, these imperfect crystals can more easily reorganize into fibrillar crystals than the lamellar crystals in AC and SC.

Stress–Strain at 25°C

Results for the room temperature tests are shown in Figure 5. Relative film behavior is the same as for the high temperature test. However, the stresses

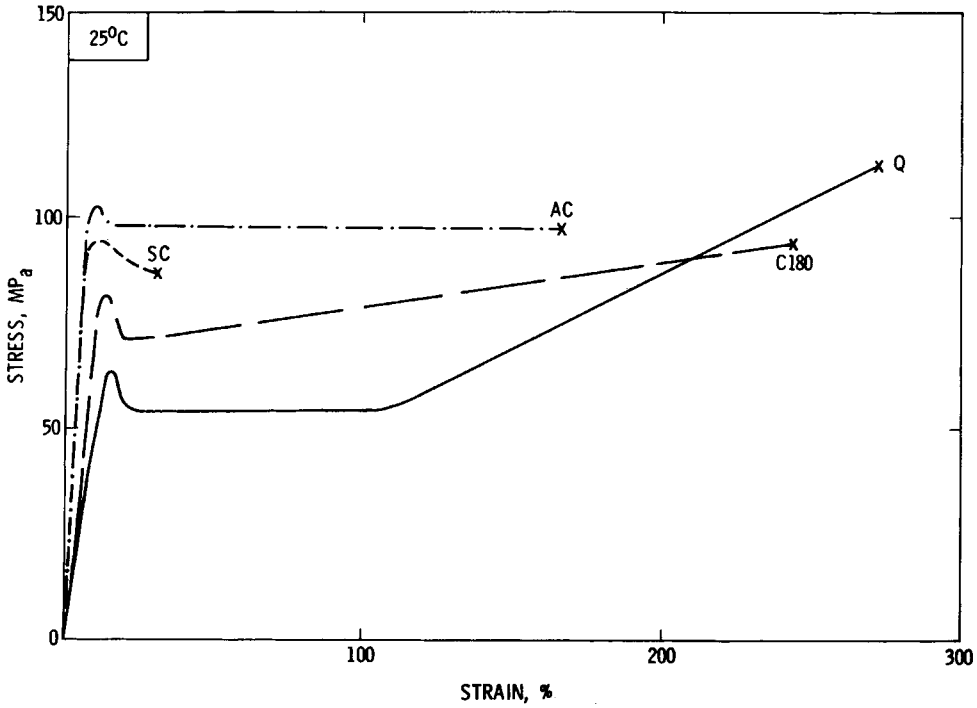

Fig. 5. Engineering stress–strain response of PEEK films drawn at 25°C.

associated with yield and neck formation in C180 are reduced at this temperature relative to the melt-crystallized films. The semicrystalline films require a greater stress for yield and for neck propagation than the amorphous film. Breaking strains decrease with increasing crystallinity as in the 125°C test.

From Figure 5, we see that the yield stress of Q at 25°C is nearly twice its value at 125°C. After yield, a neck forms and runs completely to the grips. The film then begins to harden at 100% strain. Fracture occurs at about 270% strain.

AC and C180 once again exhibit surprisingly tough behavior. AC draws to 165% strain with no evidence of strain hardening. The neck propagates at a stress level that is nearly double that of the amorphous film. Thus, in the range of strains below the breaking strain of 165%, the AC film is most tough.

C180 has stress–strain behavior between that of the Q and AC films. C180 yields and the neck propagates at an intermediate stress level with strain hardening beginning almost immediately after yield. The breaking strain of 243% is quite close to that of the Q film, making C180 a relatively tough semicrystalline film.

The trends seen during room temperature drawing support our previous interpretation that the lamellar crystals in the melt-crystallized films act to prevent hardening of the film after neck formation. AC draws at uniform stress level, whereas C180 evidences strain hardening throughout the necking period.

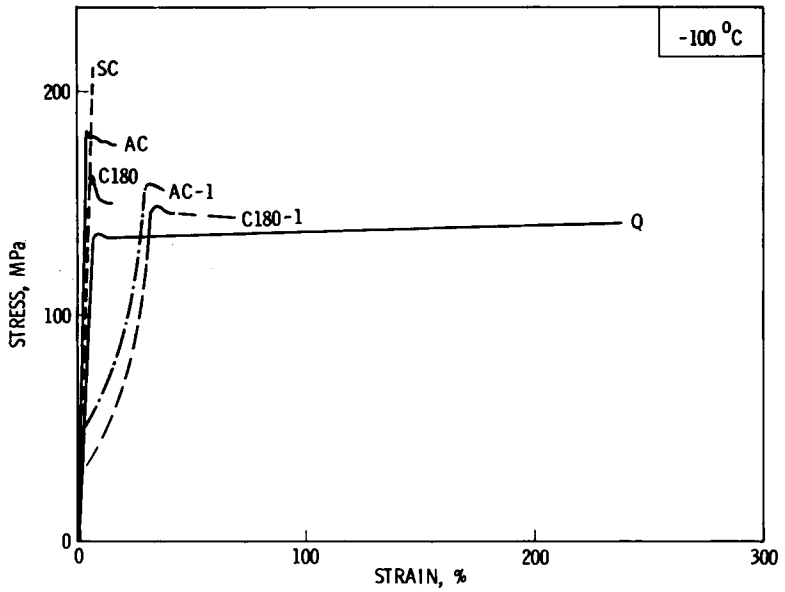

Fig. 6. Engineering stress–strain response of PEEK films drawn at −100°C. See text for explanation of sample code for AC and C180.

Stress–Strain at −100°C

Stress–strain behavior of the four films drawn at −100°C is shown in Figure 6. Two different behaviors are shown for the AC and C180 films and this will be discussed in more detail. Film Q had a yield stress of 132 MPa at 7.7% strain, followed by a very slight drop in stress level before forming a long neck. Little strain hardening was evidenced, the breaking stress of 142 MPa being only slightly greater than the yield stress. As the temperature is decreased below the glass transition, the stress for neck formation increases. At this low temperature, Q can still be drawn to over 230% before failure. None of the semicrystalline films were comparable in toughness to the Q film, even in the low strain region.

The slowly cooled film SC was very hard, withstanding a stress of over 200 MPa before breaking at low strain level of 7% without yielding. The SC films usually exhibited the brittle behavior shown in Figure 6. However, one of four SC films tested at −100°C yielded, then broke shortly beyond yield.

The AC and C180 films again had behavior intermediate between the amorphous and slowly cooled films. Both films showed two distinct yield points when a first batch of films (four to six samples of each type) was tested. The stress–strain response in Figure 6 is labeled C180-1 and AC-1 for films that exhibited the double yield. A low strain yield point at 1–2% was followed by an irregular rise in stress. (Irregularity is not visible because of the ordinate scale in Fig. 6.) The second yield point occurred at about 30–40% strain after which a short neck formed. The AC-1 sample failed shortly after the second yield point, while C180-1 could be drawn to about 80%. A second batch of AC and C180 films showed only a single yield, and these are labeled C180 and AC

in Figure 6. All the films in this set broke at relatively low strains, compared with the films exhibiting double yield behavior. The single yield samples shown in Figure 6 broke at 21% (AC) and 11% (C180).

To determine the true yield stress and strain for these samples, we note that the first yield point in C180-1 and AC-1 occurs at a low strain level, and is preceded by a linear Hooke's law region. However, the yield stress is much too low by comparison to the trends seen at higher temperature. The second yield point in AC-1 and C180-1 occurs at nearly the same stress level as the yield in AC and C180, but at too great a strain. Thus, we conclude that the true yield stress lies above 150 MPa, and the true yield strain is not greater than about 12% for both AC and C180. We attribute the apparent double yield behavior to an inhomogeneous deformation process, possibly the result of voids remaining in the sample after compression molding. Voids would act as stress concentrators and the material surrounding a void could yield by a slip-and-stick mechanism. This would account for the highly irregular stress–strain behavior between the two yield points.

Changes in Structure after Drawing

Density

After fracture we examined the density in the drawn and undrawn regions of the samples. Results are listed in Table IV for three different sample regions: undrawn, neck (n), and center (c). Densities of the undrawn polymer correspond to crystallinities shown in Table I, column 1. The densities in the n material were measured on samples cut from necked down portions, which had greatly reduced cross-sectional area compared to the undrawn sample. Material in the n section had been subject to yield, necking, and, when it occurred, strain hardening. In several cases, no neck was formed (see, for example, SC at $-100°C$), or the neck formed but did not run completely to the grips before failure occurred. In the latter case, the neck was small compared to adjacent stressed material. It was possible in these instances to cut samples from material in the center (c region) between the grips. This material was deformed homogeneously compared to that cut from the necked portion of the sample, and had nearly the same cross-sectional area as the undrawn material.

From Table IV we see that neck formation increases the density of the amorphous Q sample at all test temperatures. As temperature of drawing increases, the Q samples could be drawn to greater extensions. The density increased correspondingly as a result of increased chain packing. Necks in the Q samples ran completely to the grips before failure, so that no center regions could be obtained for these films.

In C180, the density in the neck region is reduced from that of the undrawn material. Though the density increases with increasing drawing temperature in the same way that the Q film density increased, the density in the neck was still much lower than that of the undrawn material. Even at 125°C, with a very long strain-to-break of 472%, the density of C180 films did not reach that of material before drawing. In fact, the density in the neck of C180 was lower than the density in the amorphous Q film which had about the same resultant strain (Q was drawn to 496% without breaking). Thus at comparable strain

TABLE IV
Density Changes in PEEK after Drawing

Sample	Drawing temperature (°C)	Area tested[a]	Density[b] (g/cm^3)
Q	—	Undrawn	1.265
	125	n	1.287
	25	n	1.278
	−100	n	1.273
C180	—	Undrawn	1.291
	125	n	1.281
	25	n	1.279
	−100	c	1.291
	−100	n	1.278
SC	—	Undrawn	1.300
	125	c	> 1.314[c]
	125	n	1.278
	25	c	> 1.314[c]
	25	n	1.2614 – 1.273
	−100	c	> 1.314[c]
AC	—	Undrawn	1.302
	125	n	1.282
	25	n	1.272
	−100	c	1.302
	−100	n	1.273

[a] n = necked down region; c = center region adjacent to neck.
[b] Measured at room temperature.
[c] These samples sank in a column whose maximum density was 1.314 g/cm^3.

levels, this semicrystalline film density is lower than that of the (now-drawn) amorphous film. If we now consider the center region of C180-1, we see that at −100°C the density in the center is the same as the undrawn material. Note from Figure 6 that this sample yielded initially at about 30% before the neck formed. Material from the center section experienced 30% strain, with no apparent change in density.

Very similar behavior is observed in the AC-1 film. At −100°C, neck formation results in decreased density compared to undrawn material. But density remained the same in the center section, in material that was strained to about 27% before yield and necking occurred. This comparison of the center and neck densities is quite remarkable, since, in this sample, the neck was very short. The second yield point occurred at 27% strain, while the breaking strain was only 39%. Even formation of a very short neck in the semicrystalline sample resulted in significant decreases in the density. At higher temperature the density increased with neck extension, but once again never reached the density of the original undrawn material. Because of the long necks formed at higher temperature, it was not possible to obtain center-region densities for either AC or C180 films.

The SC films, slowly cooled from the melt, were the least tough at all test temperatures. Only at or above room temperature did neck formation occur. The density in the neck region decreased for SC films just as it did for the other semicrystalline films. At 25°C, a very small neck formed, and this was

cut into three density specimens. Density varied greatly in these pieces, from 1.2614 g/cc through 1.265 g/cc, to 1.273 g/cc. The most highly drawn portion (smallest cross section) had the lowest density. The necked down region closest to unnecked, or center, material had the greatest density. The most highly drawn neck region is seen to have a density less than that of the undrawn amorphous material, a result that could be explained if voids are formed in the neck region. All densities from the center section of stressed but unnecked material were much greater than the density of the SC film before drawing. These samples sank in a column with a maximum density of 1.314 g/cc.

Results of density measurements on drawn samples can be summarized as follows. In the neck region, density in the Q film is greater than the undrawn Q material. This is due to closer packing of the amorphous chains. In all of the semicrystalline films, however, the neck density is lower than that of undrawn material. Necking in these films results in the destruction of the crystal structure and/or void formation. Wide angle X-ray scattering from the necked region in a C180 film showed no distinct crystalline reflections remaining after the sample was strained to 80%. Only very broad reflections remained, centered at scattering angles of 19° and 14°. The same result was obtained in either equatorial or meridional scans, though the peak intensity at 14° was greater in the equatorial scan. Semicrystalline films drawn at temperatures below the glass transition will experience an apparent loss of crystallinity (decrease in density) in the neck region.

Adjacent material in the c region experiences homogeneous preyield deformation, but does not neck. In AC-1 and C180-1 at −100°C, no change in density is observed, leading to the conclusion that microvoiding does not occur before yield. In film SC, the c-material density increased over the undrawn film. Since void formation is not a competing process in the c material, we conclude the densification can occur before yield in the SC films, at all three drawing temperatures.

Fracture Surfaces

In Figures 7(a)–(i), scanning electron micrographs of the fracture surfaces are shown for the toughest films tested. Film Q is shown in Figures 7(a)–(c), C180 in Figures 7(d)–(f), and AC in Figures 7(g)–(i). Drawing temperatures are −100 (top row), 25 (middle row), and 125°C (bottom row). The surface of amorphous film Q [Figs. 7(a)–(c)], is relatively smooth at all drawing temperatures. Large scale roughness is seen only in Figure 7(a), which pictures the region near a flaw which initiated the fracture. Separation of surfaces is accompanied by fibrillation in Q films, as seen in Figures 7(a) and 7(c). At room temperature, neither surface separation nor fibrillation were observed, and a more brittle fracture is suggested. Since Q films were toughest at all test temperatures, the appearance of a relatively smooth fracture surface may seem to contradict the tough nature of these films. However, Q films experienced strain hardening at the higher test temperatures, and this would result in a more brittle material. During fracture, the cross-sectional area decreases as the crack propagates, and local regions can experience much larger stresses.

Fig. 7. Scanning electron microscope pictures of fracture surfaces of Q (a–c), C180 (d–f), and AC (g–i). Drawing temperatures were −100 (top row), 25 (middle row), and 125°C (bottom row).

Fibril formation indicates regions in which large local plastic deformation occurred, such as in Figures 7(a) and 7(c) where the surfaces have pulled apart.

Both C180 and AC, shown in Figures 7(d)–(f) and 7(g)–(i), respectively, had rough-textured fracture surfaces at all temperatures. Fibrils formed in all cases and are associated with separation of surfaces, as in the Q films. At −100°C, both C180 and AC had rough surfaces indicative of a more ductile failure. The roughness decreases at room temperature for C180, and large scale separation occurs. At 125°C, two distinct fracture modes are indicated in the fracture surface of C180. Part of the sample failed in a ductile mode forming a highly irregular surface with large scale of roughness. An adjacent region of fine ridges, which run approximately in the film thickness direction, indicates a somewhat more brittle slip-and-stick type of failure. Similar fine ridges can be seen in the fracture surface of AC [Fig. 7(i)] at the same temperature. The generally smooth appearance suggests a more brittle fracture at 125°C for both C180 and AC. However, AC did not strain harden during drawing, and the appearance of the fracture surface may be due to the already large stresses imposed on the material during neck formations.

CONCLUSIONS

Thermal history imparted to PEEK films during processing affects the tensile properties of the material below the glass transition. Fast quenched amorphous films are most tough, draw to greatest strain before rupture, and undergo densification during necking. At the lowest test temperature of −100°C, these films had the best ultimate mechanical properties. At higher temperatures, the semicrystalline films AC and C180 had properties that compared favorably with the Q films. Their breaking strains were large, and in the region of low strain, these films were tougher than the Q film. The slowly cooled films exhibited poor mechanical properties at all test temperatures.

We recommend the air-cooled films for best overall performance. Their simple processing history gives AC films an advantage over the Q and C180 films which must both be quenched from the melt. The air cooling treatment results in a high degree of crystallinity and crystal perfection, which impart toughness to the films in the post-yield region. These films have the best performance for neat resin applications between room temperature and the glass transition. Further studies are underway to correlate neat resin properties with those of PEEK aromatic polymer composites having similar thermal histories.

Discussions with Drs. Muzaffer Cizmecioglu and Robert Fedors are greatly appreciated. The research described in this paper was performed by the Jet Propulsion Laboratory, California Institute of Technology, while the principal author held an NRC-NASA Resident Research Associateship Award. Research was sponsored by National Aeronautics and Space Administration.

References

1. J. N. Hay, D. J. Kemmish, J. I. Langford, and A. I. M. Rae, *Polym. Commun.* **25**, 175 (1984).

2. T. E. Attwood, P. C. Dawson, J. L. Freeman, L. R. J. Hoy, J. B. Ross, and P. A. Staniland, *Polymer*, **22**, 1096 (1981).

3. Osamu Yoda, *Polym. Commun.*, **25**, 238 (1984).
4. M. T. Bishop, F. E. Karasz, P. S. Russo, and K. H. Langley, *Macromolecules*, **18**, 86 (1985).
5. A. J. Lovinger and D. D. Davis, *Polym. Commun.*, **26**, 322 (1985).
6. D. J. Blundell and B. N. Osborn, *Polymer*, **24**, 953 (1983).
7. P. Cebe and S. -D. Hong, *Polymer*, **27**, 1183 (1986).
8. P. Cebe, *Polym. Prepr.*, **27**(1), 449 (1986).
9. D. R. Rueda, F. Ania, A. Richardson, I. M. Ward, and F. J. Balta Calleja, *Polym. Commun.*, **24**, 258 (1983).
10. A. J. Lovinger and D. D. Davis, *J. Appl. Phys.*, **58**, 2843 (1985).
11. D. J. Blundell, J. M. Chalmers, M. W. Mackenzie, and W. F. Gaskin, *SAMPE Qu.*, **16**(4), 22 (1985).
12. D. J. Blundell and B. N. Osborn, *SAMPE Qu.*, **17**(1), 1 (1985).
13. E. J. Stober, J. C. Sefaris, and J. D. Keenan, *Polymer*, **25**, 1845 (1984).
14. D. J. Kemmish and J. N. Hay, *Polymer*, **26**, 905 (1985).
15. D. P. Jones, D. C. Leach, and D. R. Moore, *Polymer*, **26**, 1385 (1985).
16. T. Sasuga and M. Hagiwara, *Polymer*, **26**(4), 501 (1985).
17. P. Cebe, S. D. Hong, S. Y. Chung, and A. Gupta, *ASTM Special Technical Publication on Toughened Composites*, to appear.
18. J. M. Chalmers, W. F. Gaskin, and M. W. Mackenzie, *Polym. Bull.*, **11**, 433 (1984).
19. J. L. Way, J. R. Atkinson, and J. Nutting, *J. Mater. Sci.*, **9**, 293 (1974).

Received March 20, 1986
Accepted April 22, 1986